AD NUMBER

ADC011773

NEW LIMITATION CHANGE

TO

Approved for public release, distribution unlimited

FROM

Distribution limited to U.S. Gov't. agencies only; Test and Evaluation; 14 Oct 77. Other requests for this document must be referred to Commanding Officer, Naval Research Lab., Washington, DC 20375.

AUTHORITY

NRL ltr, 22 Jan 2004

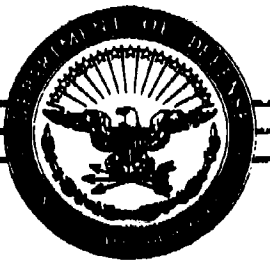

AD NUMBER

C011 773

CLASSIFICATION CHANGES

TO

UNCLASSIFIED

FROM

CONFIDENTIAL

AUTHORITY

CO NRL

DISCLAIMER NOTICE

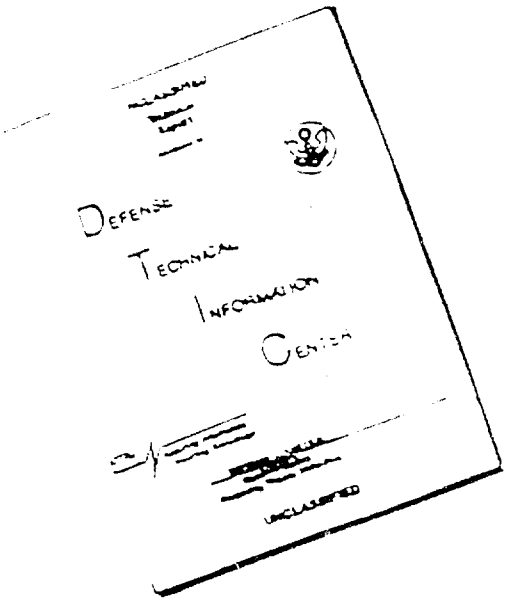

THIS DOCUMENT IS BEST QUALITY AVAILABLE. THE COPY FURNISHED TO DTIC CONTAINED A SIGNIFICANT NUMBER OF PAGES WHICH DO NOT REPRODUCE LEGIBLY.

[redacted]

NRL Memorandum Report [illegible]

PROJECT ARTEMIS
HIGH POWER ACOUSTIC SOURCE

(Unclassified Title)

A. T. McClinton, R. H. Ferris,
and W. A. Herrington

SOUND DIVISION

3 August 1961

U. S. NAVAL RESEARCH LABORATORY
Washington, D.C.

[redacted]

[redacted] T, 1205

PROJECT ARTEMIS
HIGH POWER ACOUSTIC SOURCE

Interim Report on Acoustic Performance (U)
(Unclassified Title)

NRL-MR-1205

by
A. T. McClinton
R. H. Ferris
W. A. Herrington

41 p.

3 August 1961

Electrical Applications Branch
Sound Division
U. S. NAVAL RESEARCH LABORATORY
Washington 25, D. C.

251950

[redacted]

NATIONAL SECURITY INFORMATION

Unauthorized Disclosure Subject to Criminal Sanctions

AB

DISTRIBUTION

CNO

Attention:	Op-001	1
	Op-03EG	2
	Op-07	1
	Op-31	1
	Op-70	1
	Op-714D	1

ONR

Attention:	Code 400X	11

USNEL, San Diego, California

Attention:	Technical Library	2

NAVUWTRSOUNDREFLAB

Attention:	Technical Library	1

NAVUWTRSOUNDLAB

Attention:	Technical Library	2

Hudson Laboratories, Columbia University
145 Palisade Street, Dobbs Ferry, New York

Attention:	Dr. R. A. Frosch	10

[redacted]

CONTENTS

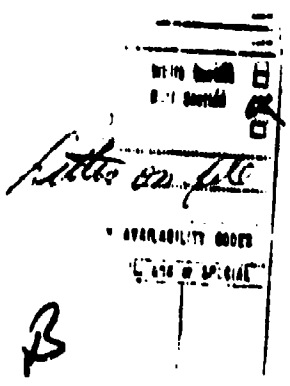

[redacted]

ABSTRACT

This report describes and presents the results of acoustic tests with the partially completed ARTEMIS source array at limited power levels. The purposes of these tests were to obtain impedance characteristics, response data and transducer displacement as a function of power, frequency and operating depth. Results indicate large variations in displacements over the face of the transducer, resulting in peak values in excess of those predicted on the basis of radiated power. A tentative maximum efficiency in excess of fifty percent was obtained subject to an assumed directivity pattern and hydrophone sensitivity. Spurious mechanical resonances were observed as evidenced by the impedance diagrams.

PROBLEM AUTHORIZATION

ONR NR 287 002 (Special)
NRL Problem Number 55S02-11

PROBLEM STATUS

This is an interim report on one phase of the project. Work is continuing.

[redacted]

INTRODUCTION

An array composed of 144 electromagnetic transducer elements was installed on the USNS MISSION CAPISTRANO (T-AG 162) for experimentation and determination of their operating characteristics. The transducer element is a type TR-11C manufactured to U. S. Naval Research Laboratory specification by Massa Division, Cohu Electronics, Incorporated. Each element is 11-1/8 inches square on the radiating faces and 11-3/4 inches deep. They are assembled in modules of 72 transducers, six elements wide by twelve elements high. Two such modules were installed on the array structure on the USNS MISSION CAPISTRANO. The installation is shown in figure 1.

The 72 transducer elements in each module are grouped in twelve rows of six elements each. The six elements in each row are connected together in series electrically with the twelve rows connected in parallel. The two modules are then connected in parallel in an oil-filled junction box. Thus the array consists of 24 parallel groups of six elements in series. The dc polarising power as well as the ac power is supplied to this group.

Acoustic pressure release is applied to the rear side (opposite of side shown in figure 1) of the modules. This consists of a squash tube resonant reflector. The tubes are six feet long and extend horizontally across the back of each row of six transducers. The flattened tube is approximately six inches wide, thus covering about one-half the rear radiating surface of the transducers. The tubes are separated approximately one-half inch from the rear face of the array. In order to prevent the tubes from flattening, that is, prevent the walls from touching due to the ambient pressure, the tubes are filled with nitrogen gas from a regulated system. The regulated pressure is adjustable in the range from plus 20 pounds to plus 60 pounds relative to ambient. The maximum operating pressure of plus 60 pounds relative to ambient also occurs on raising the array to the surface, since the pressure relief valve is set for 60 pounds.

EXPERIMENTAL PROCEDURE

Experimental work with these two modules in an array was conducted during the period of May and June 1961. Two operating areas were used.

[redacted]

One was in the Chesapeake Bay near Cape Charles, Virginia, in a water depth of 90 feet. The maximum possible operating depth to the center of the two modules was approximately 40 feet. The second operating area was in the Atlantic Ocean northeast of the Bahamas at approximately 28° N. 74° W.

Power to the array was supplied by a 60 kilowatt diesel-driven dc generator for polarization and by either of two amplifiers. A 200 watt McIntosh was used for lower current observations (1.5 amperes and less) and a 1300 kilowatt Ling amplifier for high values of current. Wave form of the ac signal was sinusoidal in all instances. The pressure release system was operated at approximately 30 pounds above ambient.

Instrumentation was provided to measure dc polarization current, ac current, voltage, power and frequency with an oscilloscope to monitor wave form. Two hydrophones were mounted near the array to monitor the acoustic output. One was mounted on a boom which placed the hydrophone 28 feet on the center line in front of the array. The second hydrophone was also on the center line but 17 feet in back of the array. This hydrophone was at the furthest point on the array structure back of the two modules.

Two accelerometers were also employed to obtain data on the amplitude of movement of the transducer radiating face. These accelerometers were screwed into the taped hole normally used for the lifting eye. Since this hole is on the rear face of the array, as the elements are normally installed, provisions were made to reverse two transducer elements, thus putting the taped hole on the front radiating face. The transducers thus reversed were the first one from the left, second row from the top of the left hand module as seen from the front of the array, and the sixth one from the left, seventh row from the top of the left hand module. These accelerometers have been designated A_2 and A_1 respectively.

All instrumentation was calibrated before and after the experiments with the exception of the monitoring hydrophones. Data presented herein are based on calibrations obtained in shallow water. These units are being recalibrated in deep water where greater precision

can be obtained. Data involving acoustic power output, efficiency and front-to-back ratio could be changed in magnitude by this calibration but relative levels are expected to be valid.

The accelerometers have been calibrated both in air and in water. The latter has involved both an acoustic and non-acoustic ambient. The output of these units was not affected by these ambient conditions.

Prior to conducting the experiments, an activity check was made in air on each element in the array of 144 elements. The purpose of this test was to determine that all transducers were operating and not defective and that all units were moving in phase indicating proper electrical connections.

The primary purpose of the experiments was to obtain the conventional impedance characteristics and response curves. In addition, data were to be obtained on operating efficiency, the influence of input current and frequency, the front-to-back ratio, and depth effects. Early results indicated the necessity of measuring transducer amplitude to determine this value with respect to input current, radiated power and position in the array.

Tests where all instrumentation described above was employed were limited to a maximum depth of 360 feet. Observations were made at 400 feet depth. However, due to cable length limitations, these did not include the accelerometers.

EXPERIMENTAL RESULTS

All data presented herein are the total characteristics of the 144 element array unless otherwise noted. Input values of ac or dc current are always to the entire array. If it is desired to obtain the value per transducer element, the value given should be divided by 24 which is the number of parallel paths. The polarizing current used throughout was 240 amperes or ten amperes per element. AC current was varied from a minimum of 0.5 amperes in air to a maximum of 40 amperes in water.

The results of impedance measurement with the array in air are presented in figures 2 and 3. The resonant frequency, f_r, is approximately 458.5

cycles per second with an impedance $\dot{Z}$ = 200 + j25 ohms. This compares with the average value of the data for a single element in air of f_r = 450 cps and $\dot{Z}$ = 1000 + j35 ohms. The mechanical Q for the array is Q_m = 41.7, whereas it varied from 25 to 55 for the single elements in air.

These curves were repeated in water at a depth to the center of the array of 36 feet. Vector impedance diagrams are shown in figures 4 and 5 for ac currents of 0.5 ampere and 1.5 amperes respectively. Insufficient number of frequencies were used to permit drawing the optimum "circle" through these points. However, it appears that a number of resonances exist. This is more clearly evidenced in the impedance plot at 1.5 amperes in figure 6. The best estimate for the impedance is $\dot{Z}$ = 25 + j20 ohms with resonance at f_r = 420 cps.

Because of the proximity of the transducer elements to the surface and bottom, evaluation of these secondary resonances from figure 6 may be somewhat in error. Additional data were obtained of the array impedance in the ocean in a water depth in excess of 2400 fathoms with the depth to the center of the array of 90 feet and 400 feet. The results at 15 amperes input for these depths are shown on figures 7 through 10. It is evident from these data that numerous secondary resonances occur between 340 cps and 440 cps. Without a larger number of data points in this area one can only speculate on the exact shape of the impedance characteristics of figures 8 and 10.

A general improvement in the impedance curve was noted at the higher current level. This is to be evidenced in the vector impedance diagram of figure 11 and in particular in the impedance plot of figure 12. It is to be noted here that two prominent areas of secondary resonances are present, one in the vicinity of 370 cps and a second at 430 cps. The resonant frequency, f_r, is at approximately 405 cps and the impedance $\dot{Z}$ = 36 + j21 ohms.

The impedance data shown in figures 13 and 14 should compare with that of figures 11 and 12. However, it will be noted that there is a shift toward a higher frequency and the secondary resonance at the higher frequency is more pronounced. This trend may be due to damage to a few of the elements in the array. The damage which was ascertained on completion of the tests was in the form of broken springs. This has the effect of raising the resonant frequency of the damaged element and thus could have produced the effect noted here.

It is of interest to compare this data from figures 11 and 12 obtained at 30 amperes and 400 foot depth with impedance data taken at 40 amperes, 39 foot depth. The same general location of secondary resonances again may be seen from figures 15 and 16. It will be observed, however, that resonance is at approximately 410 cps and that Z = 30 + j21 ohms.

Data from the two accelerometers were obtained at depths of 36 feet, 90 feet and 360 feet. A summary of the more significant data is presented in figures 17, 18 and 19. Data for the three curves were taken at constant current; namely 1.5, 15 and 30 amperes. It may be observed from these curves as well as from the previously discussed impedance curves that deviations from the idealized occur at certain predominant frequencies. Since amplitude should relate more exactly to acoustic power, all data obtained at 90 feet and at 360 feet depth were plotted against acoustic output power in kilowatts. These results are shown on figures 20 and 21 respectively. Each point of data has been identified as a plotted point. However, an attempt has been made to distinguish between frequencies by using several symbols with each symbol being used for points within a frequency band. In figures 20a through 20r and 21a through 21r, the transducer displacements are separated for each frequency at which measurements were made.

The dashed curves drawn on each of the figures, 20 through 21r, represent the displacement to be expected for approximately unity ρc loading of the array at the frequencies noted on the curves. A best-fit curve through the points on figures 20 and 21 indicates that this loading has not been achieved and that a better approximation of the results is obtained with 0.4 ρc loading. In general, the points would be fairly uniform about such a curve except at the higher acoustic power levels on figure 21. Here it will be noted that there is a sharp rise in the transducer amplitude.

The response curves for the array at several values of current are presented in figure 22. Deviations from an idealized smooth curve are to be noted on all of the curves. These occur at approximately 370 and 425 cps which also correspond to the frequencies of secondary resonances previously noted.

Curves of power input, output ... efficiency for the array are presented in figures 23 and 24. These values were obtained with 30 amperes at 400 feet and 360 feet depth respectively. The maximum efficiency is noted to be slightly over 55 percent and occurs near 440 cps. Deviation of the various curves from a smooth line is again evidenced with these data and it can also be seen to occur at approximately the same frequencies previously noted for the impedance characteristics and transducer displacements.

The effectiveness of the squash tube pressure release device is presented in figures 25 and 26. The front-to-back discrimination was computed from the hydrophone measurements of the transducer radiation for input currents of 5, 10, 15, 20, 25 and 30 amperes. The average of the values obtained at each frequency at 400 foot depth are plotted on figure 25. In addition, a vertical line which corresponds to the extent of the maximum and minimum values obtained at each frequency is also shown.

The characteristic deviation of this curve from a single resonant characteristic is also noted as with previous characteristics. Resonances in the response curve correspond to frequencies of approximately 350, 410 and 440 cps. Similar characteristics are to be noted in the front-to-back discrimination data on figure 26. These data are for 30 amperes and 40 amperes at 360 foot depth.

With two exceptions, the spread in front-to-back discrimination with current at any one frequency shown on figure 25 is small, indicating that within the range tested the response of the squash tube is independent of transducer current, output power or displacement of the transducer radiating face. This is best illustrated by figure 27 where front-to-back discrimination is plotted as a function of current for several frequencies.

During the period of these experiments, tests on the transducer elements indicated that failure of several elements had occurred. These failures were apparently the result of excessive deflection of the springs which were broken. The first group of damaged elements occurred at 39 foot depth when operations were conducted with current of 40 amperes with a few observations at higher values. Sixty-four elements failed in the pattern shown in figure 28.

It was as a result of these failures that accelerometers were employed to obtain information on the displacement amplitude of the radiating face. During the course of the tests with the accelerometers in place, large variations in displacements were obtained, with the majority in excess of predicted values. The array was operated on two occasions at a current of 40 amperes; the first at 400 foot depth without accelerometer data and the second at 360 feet with accelerometer data. A peak-to-peak displacement of 9.71 mils was observed for one of the transducers prior to one of its springs breaking.

Tests on the individual transducer elements after the above tests revealed 21 transducers had failed due to broken springs. In addition to these, four squash tubes had also failed. The latter failed with a fracture on the edge of the sharp radius of bend. The pattern of these failures is shown in figure 29.

With the transducer impedance and current response data obtained in these tests, an overall system response for constant voltage input to the amplifier can be computed. This computation has been made for the conditions of the amplifier matched to a 34 ohm resistive load and with a series tuning capacitor of impedance -j22 ohms. These values correspond to a complex conjugate impedance match to the transducer at 400 cps. The results of this computation are plotted in figure 30. A similar set of data with the amplifier matched to 25 + j22 ohms is plotted in figure 31. Both curves have been normalized to a zero decibel intensity on the acoustic axis at 400 cps. These characteristics indicate the response of the system to a noise signal input and can be used to determine the compensation required to produce a constant amplitude frequency spectrum over the desired frequency range.

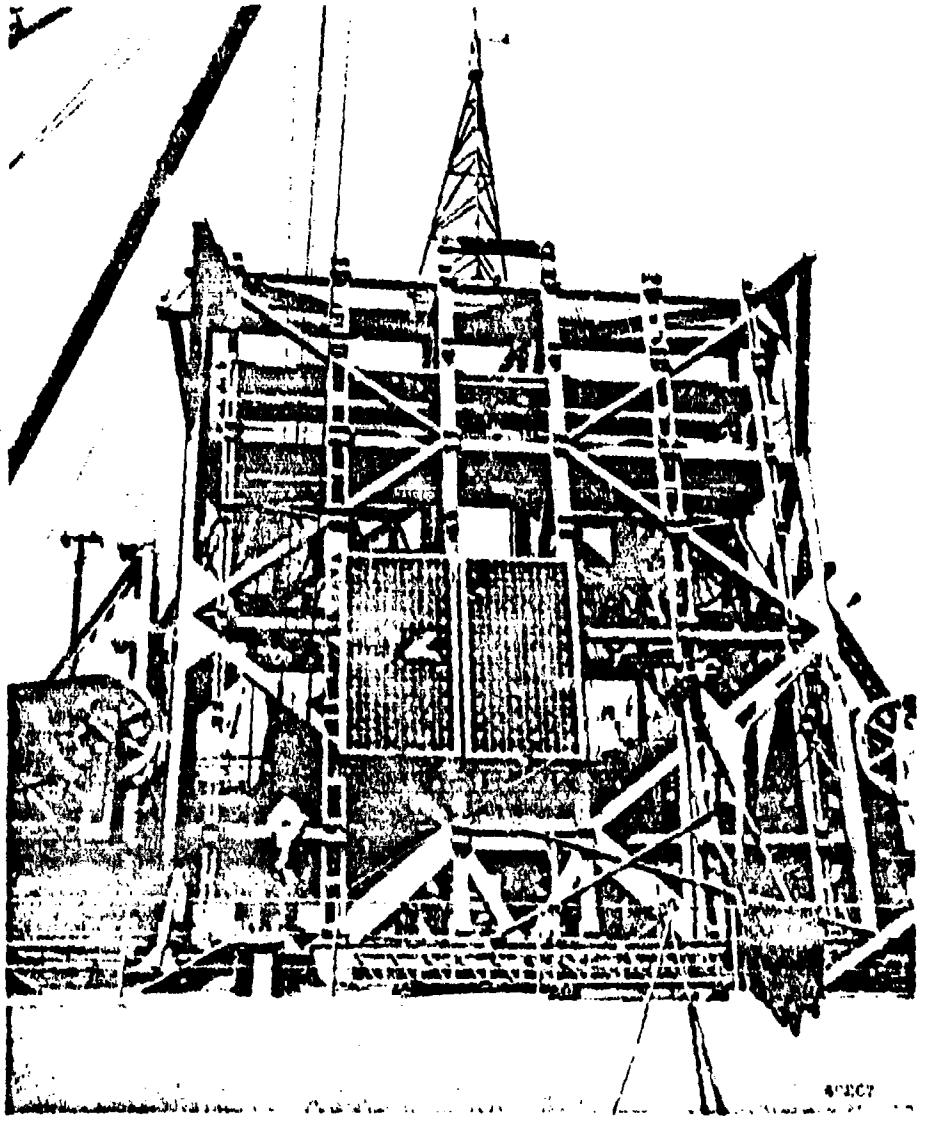

Figure 1-1. Photo of array with 2 modules

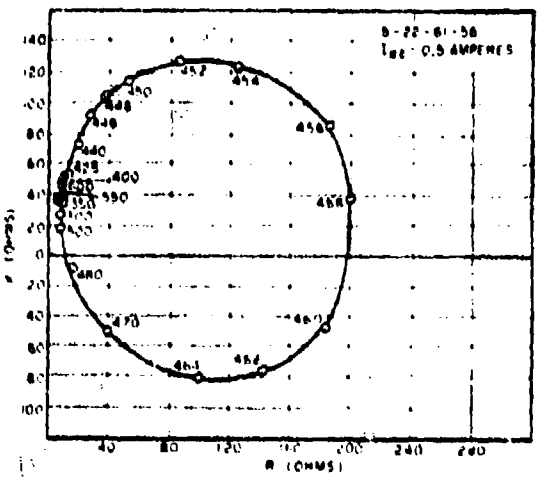

Figure 2 - Vector impedance diagram in air

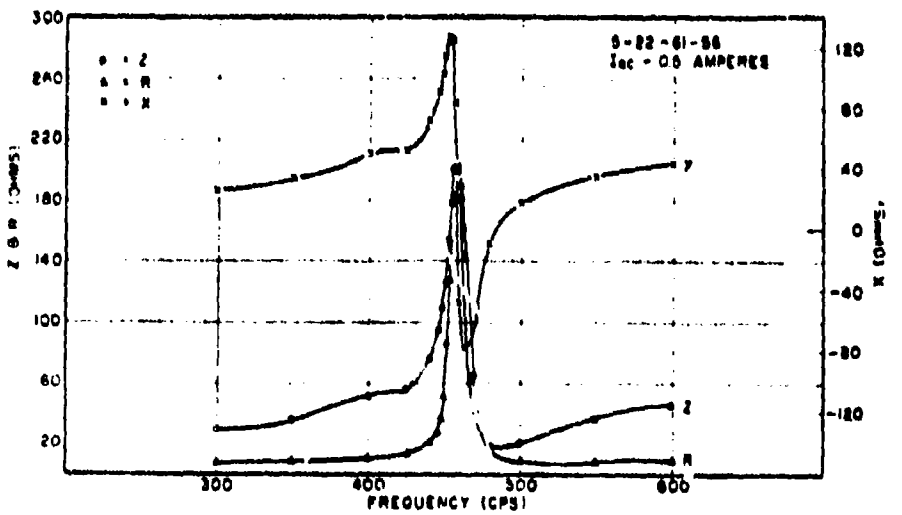

Figure 3 - Impedance characteristics in air

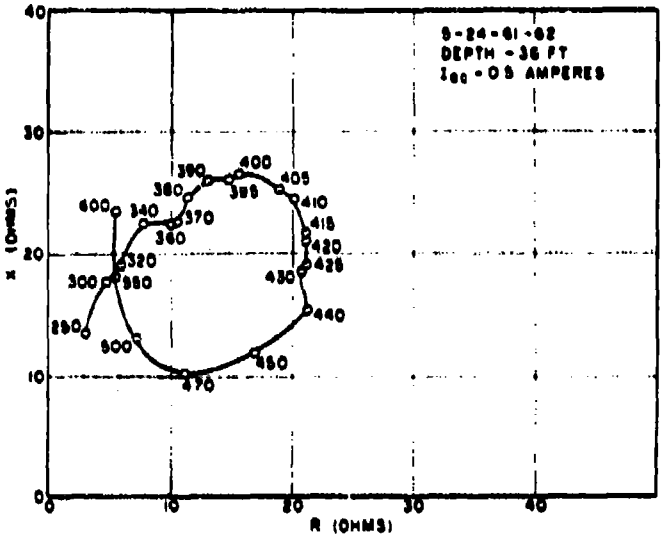

Figure 4 - Vector impedance diagram

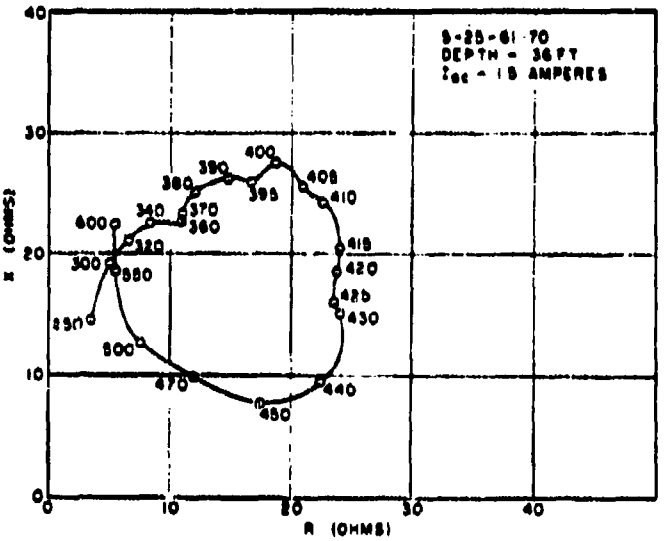

Figure 5 - Vector impedance diagram

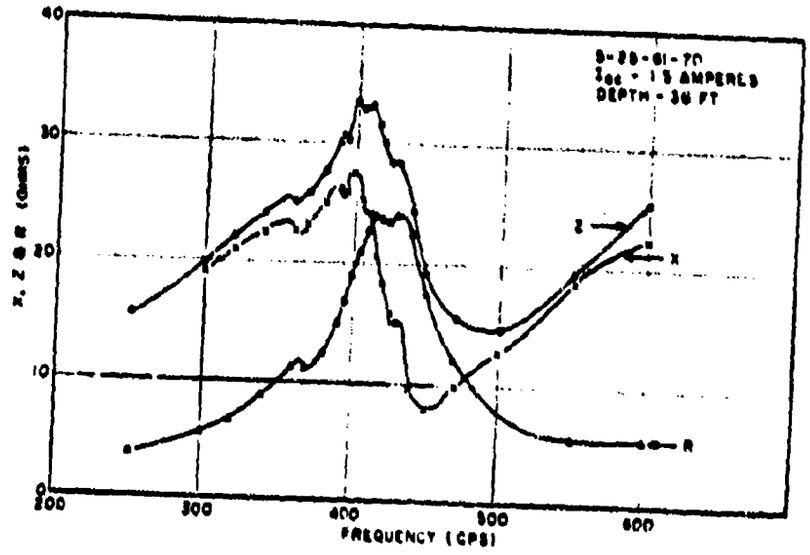

Figure 6 - Impedance characteristics

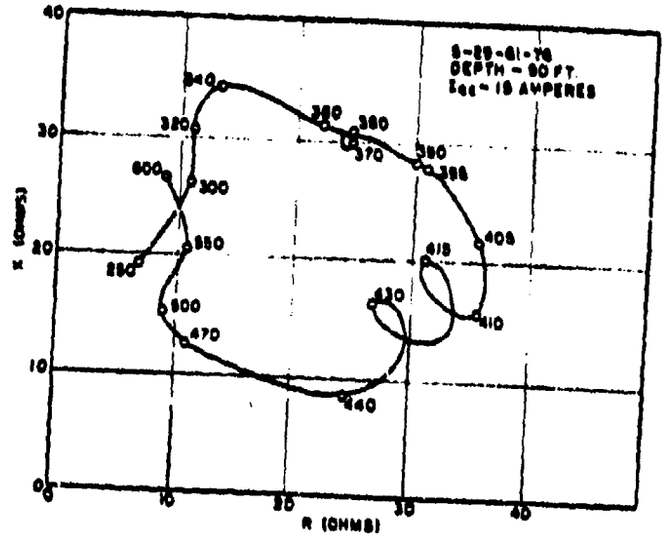

Figure 7 - Vector impedance diagram

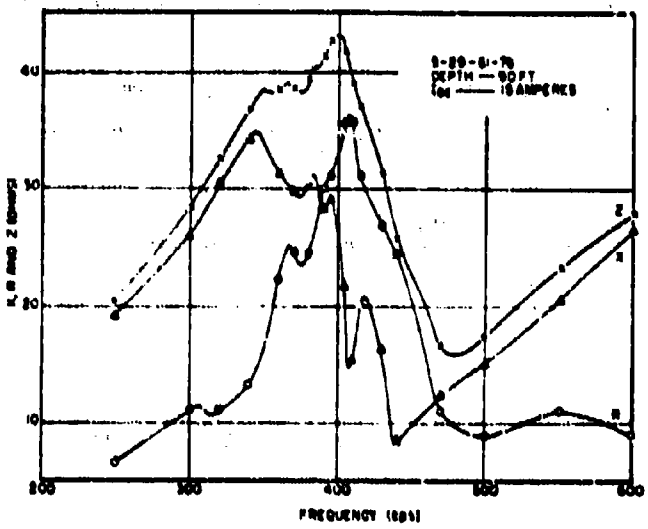

Figure 8 - Impedance characteristics

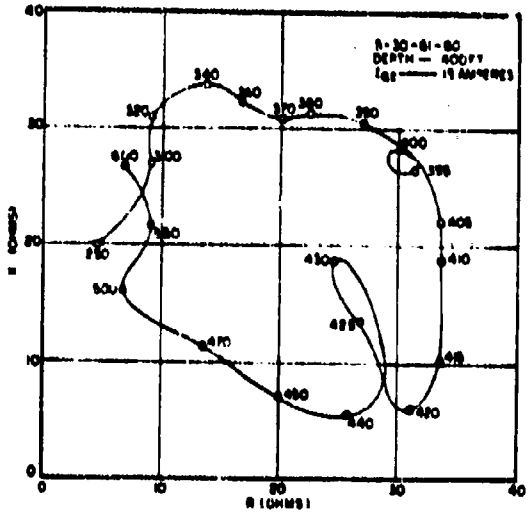

Figure 9 - Vector impedance diagram

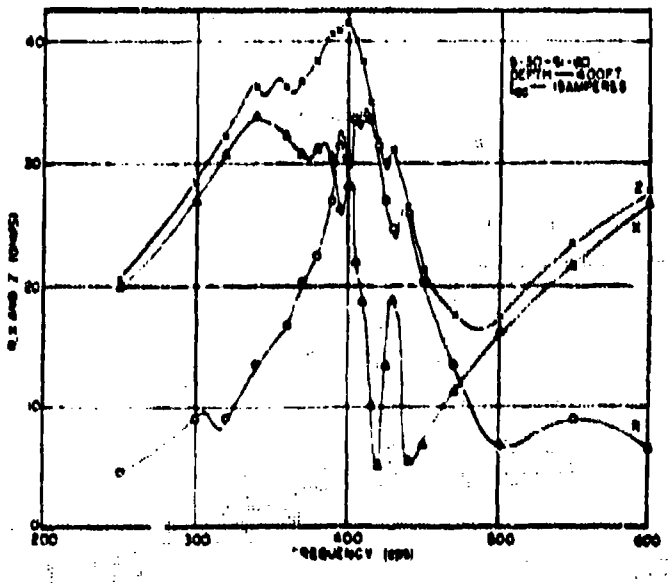

Figure 10 - Transducer impedance characteristics

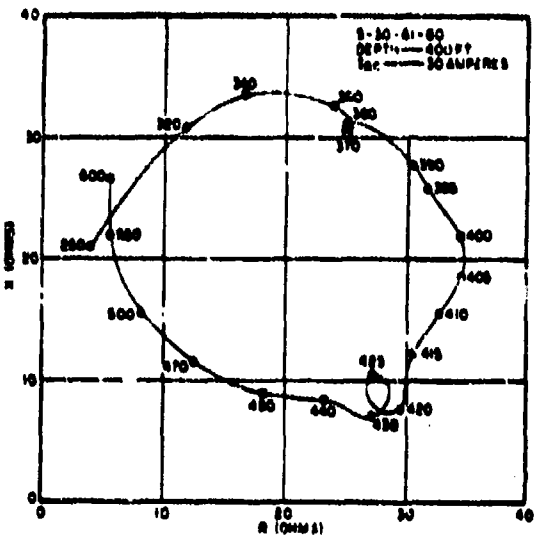

Figure 11 - Vector impedance diagram

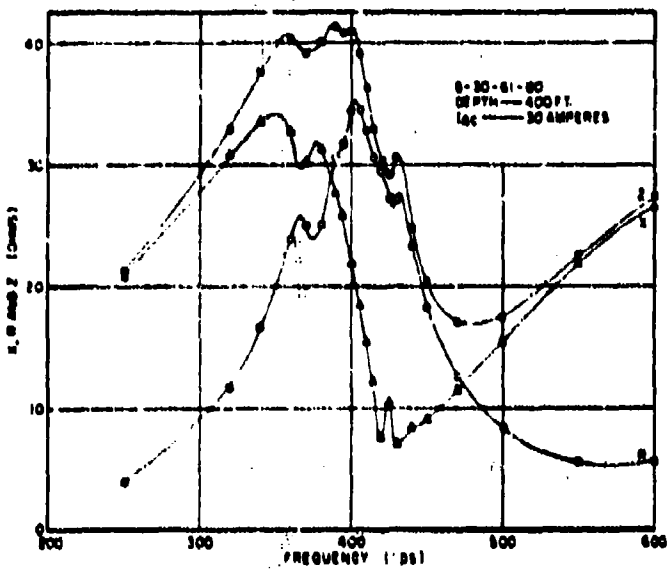

Figure 12 - Impedance characteristics

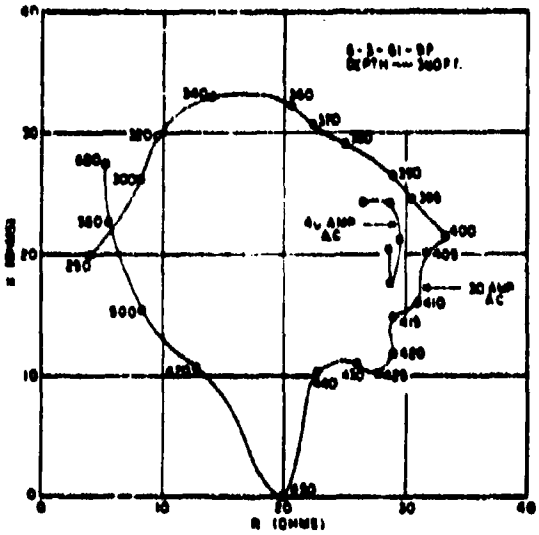

Figure 13 - Vector impedance diagram

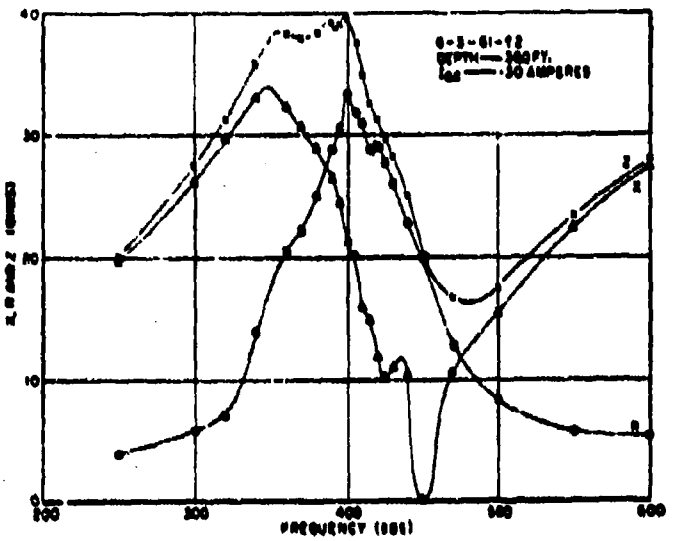

Figure 14 - Impedance characteristics

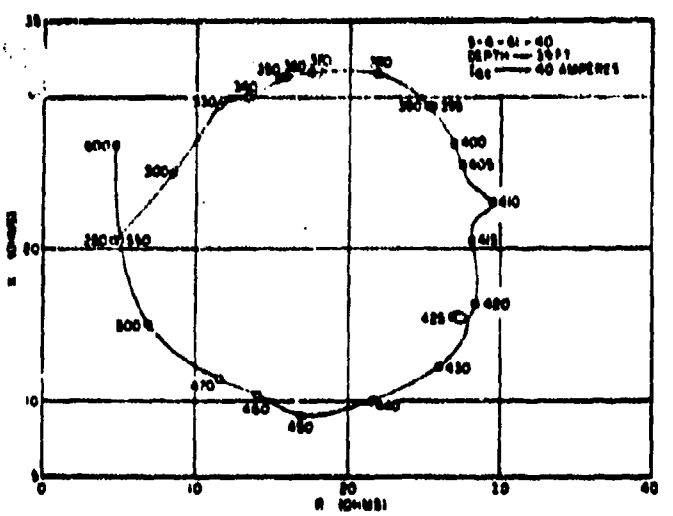

Figure 15 - Vector impedance diagram

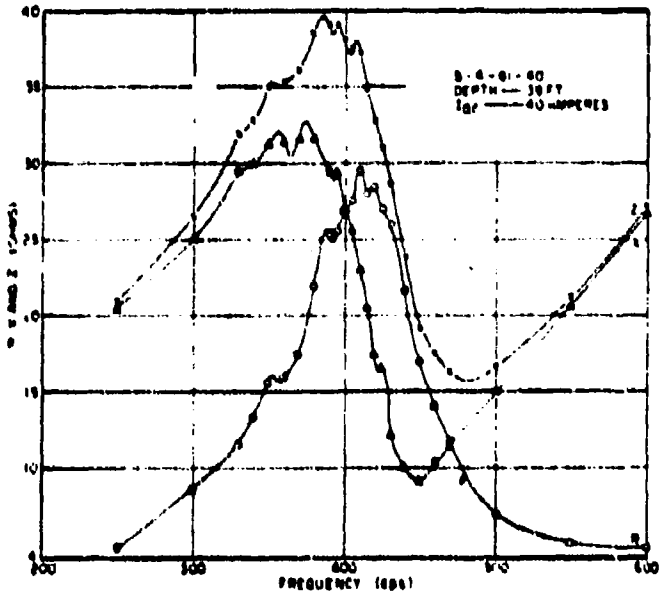

Figure 16 - Transducer impedance characteristics

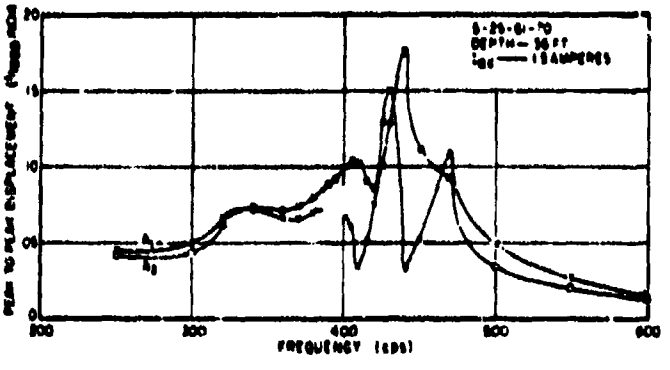

Figure 17 - Transducer displacement

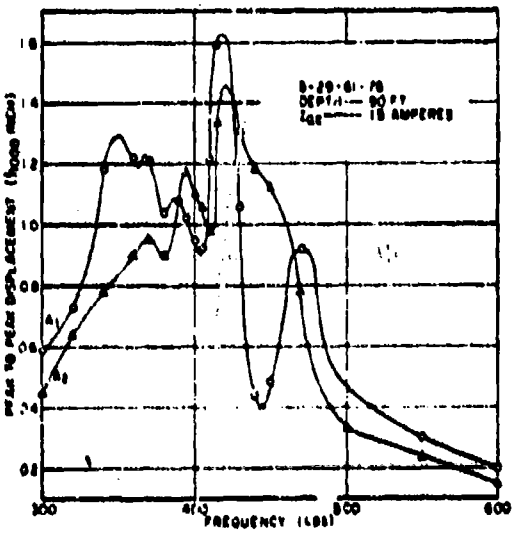

Figure 18 - Transducer displacement

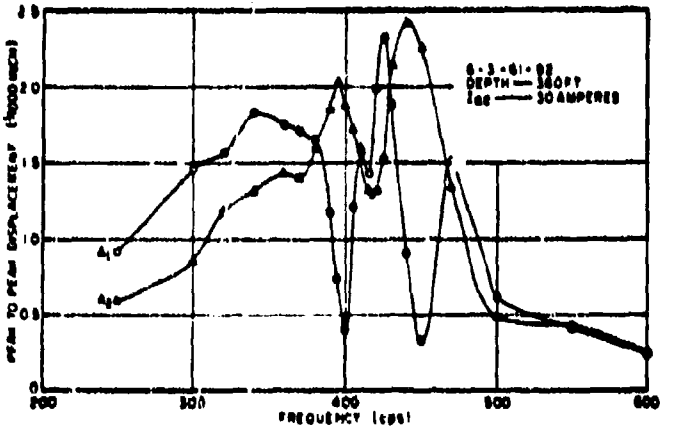

Figure 19 - Transducer displacement

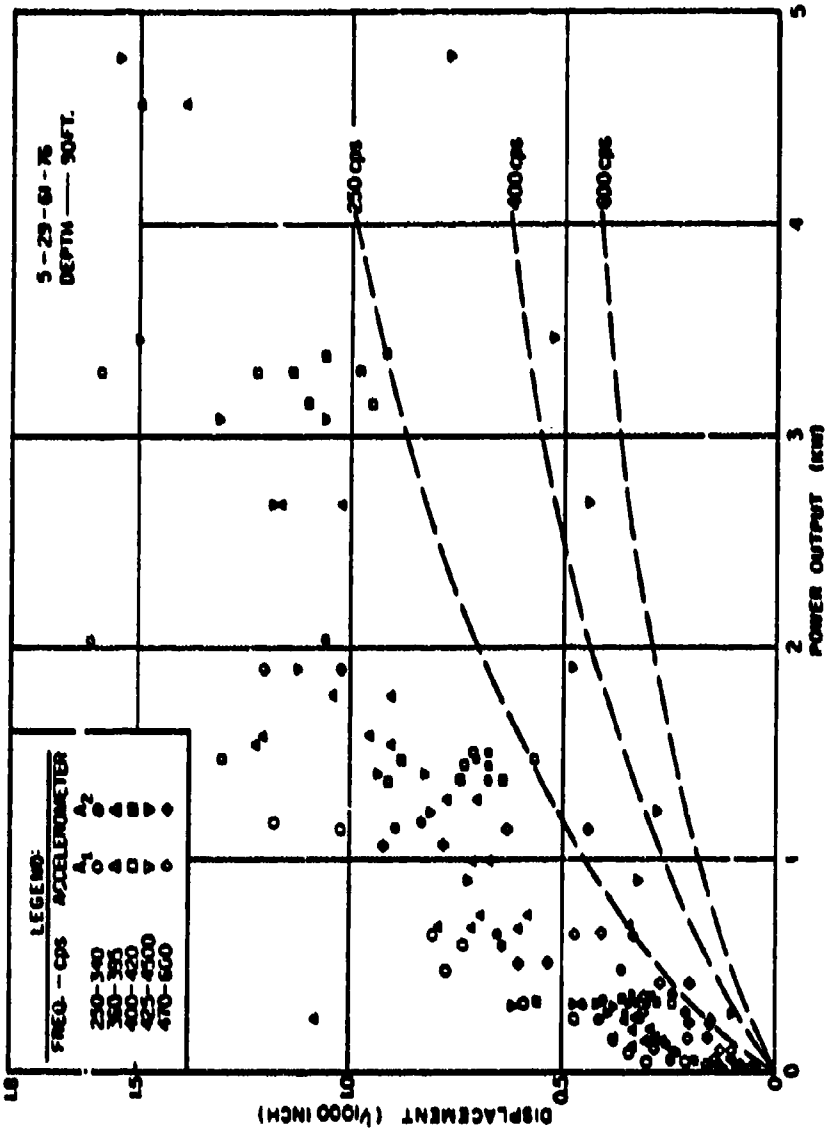

Figure 20 - Transducer displacement characteristics

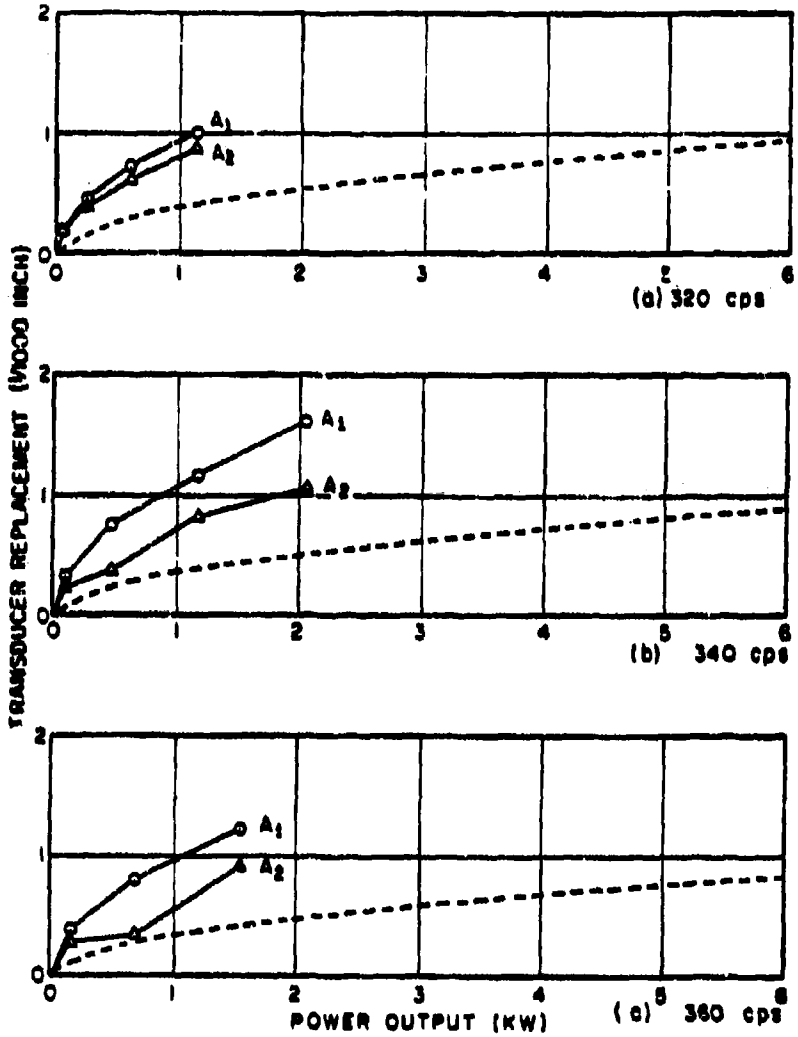

Figure 20 (Continued) - Transducer displacement characteristics

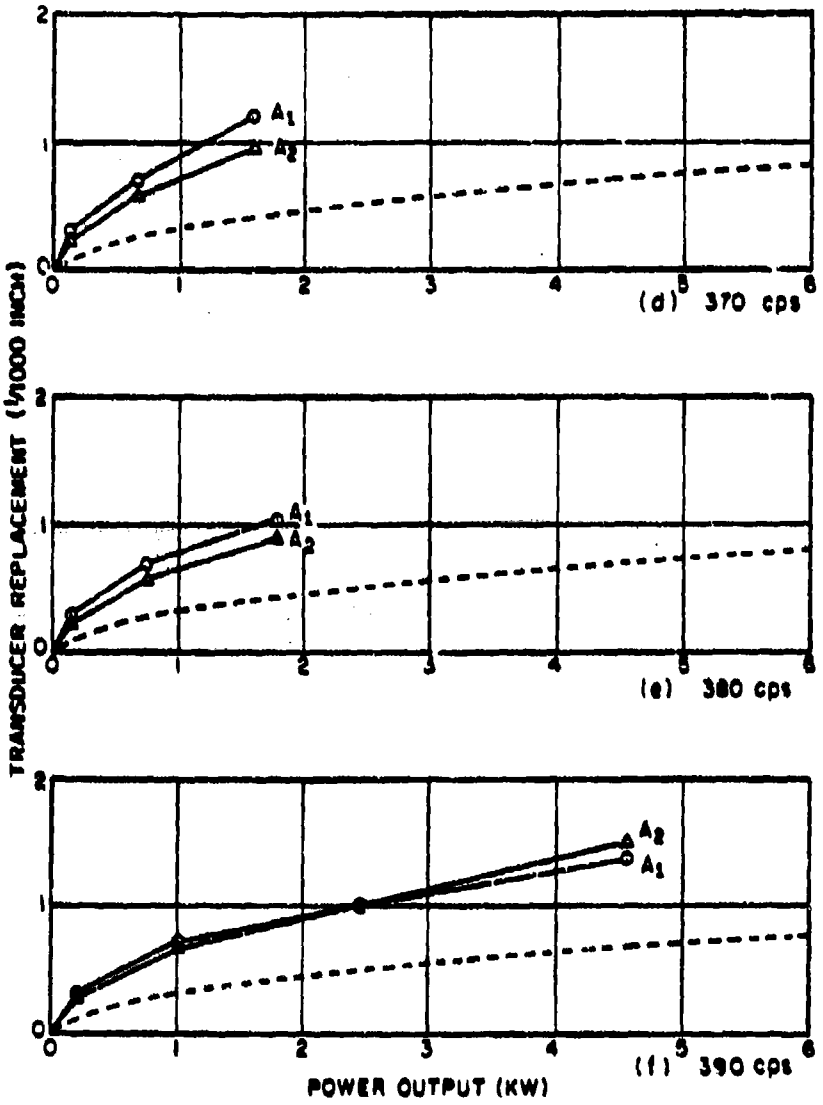

Figure 20 (Continued) - Transducer displacement characteristics

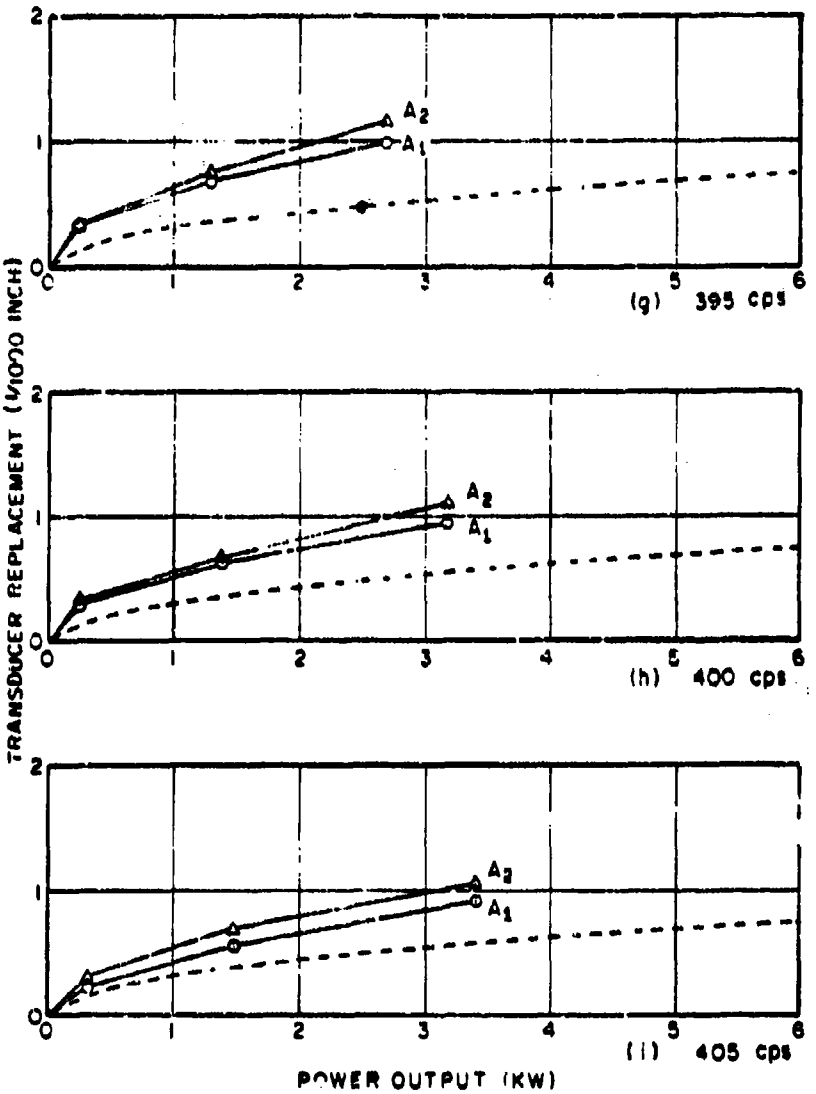

Figure 20 (Continued) - Transducer displacement characteristics

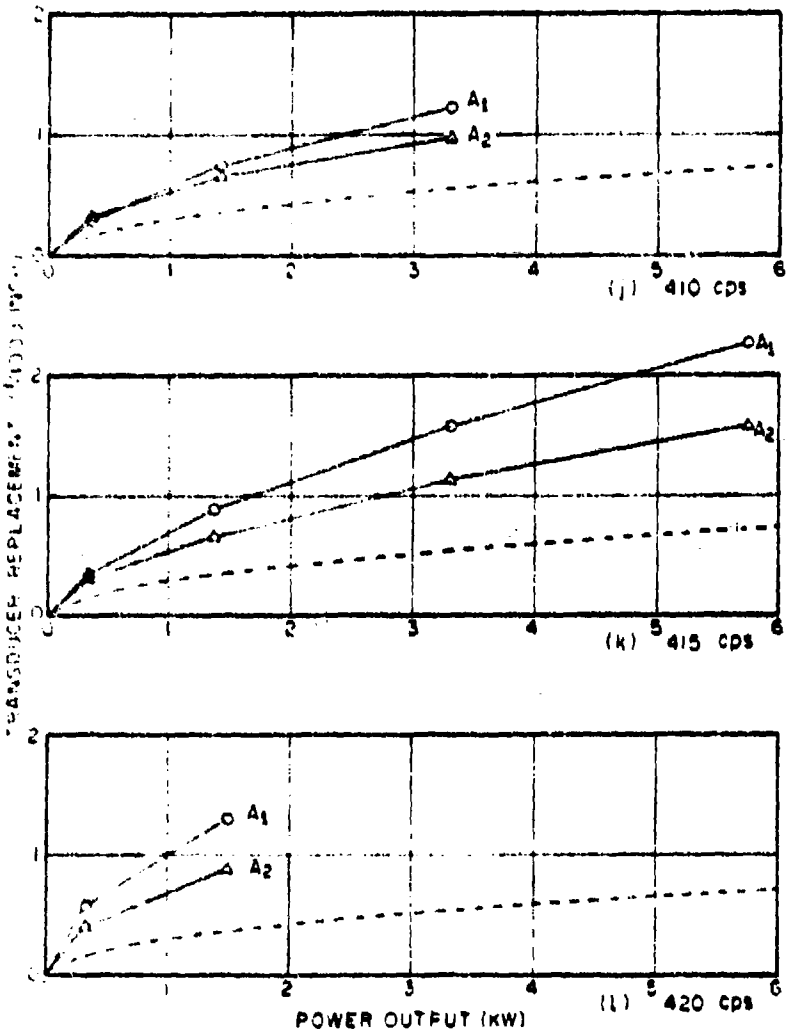

Figure 20 (Continued) - Transducer displacement characteristics

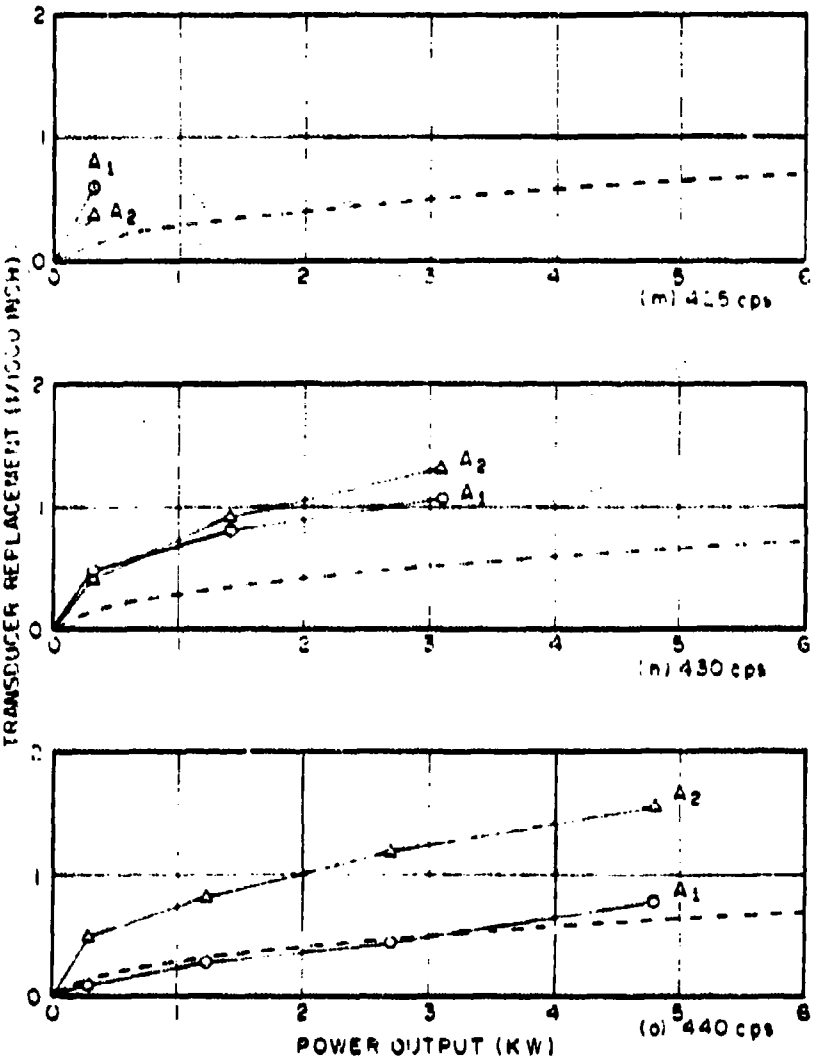

Figure 20 (Continued) - Transducer displacement characteristics

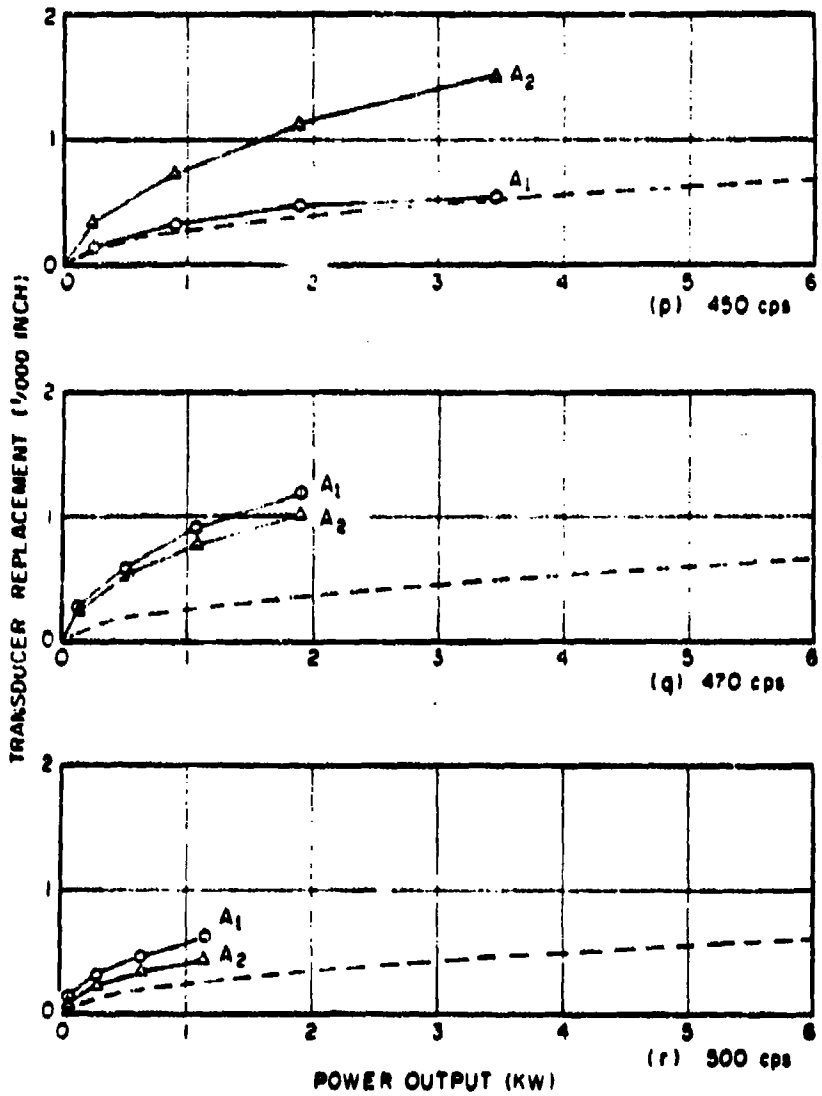

Figure 20 (Continued) - Transducer displacement characteristics

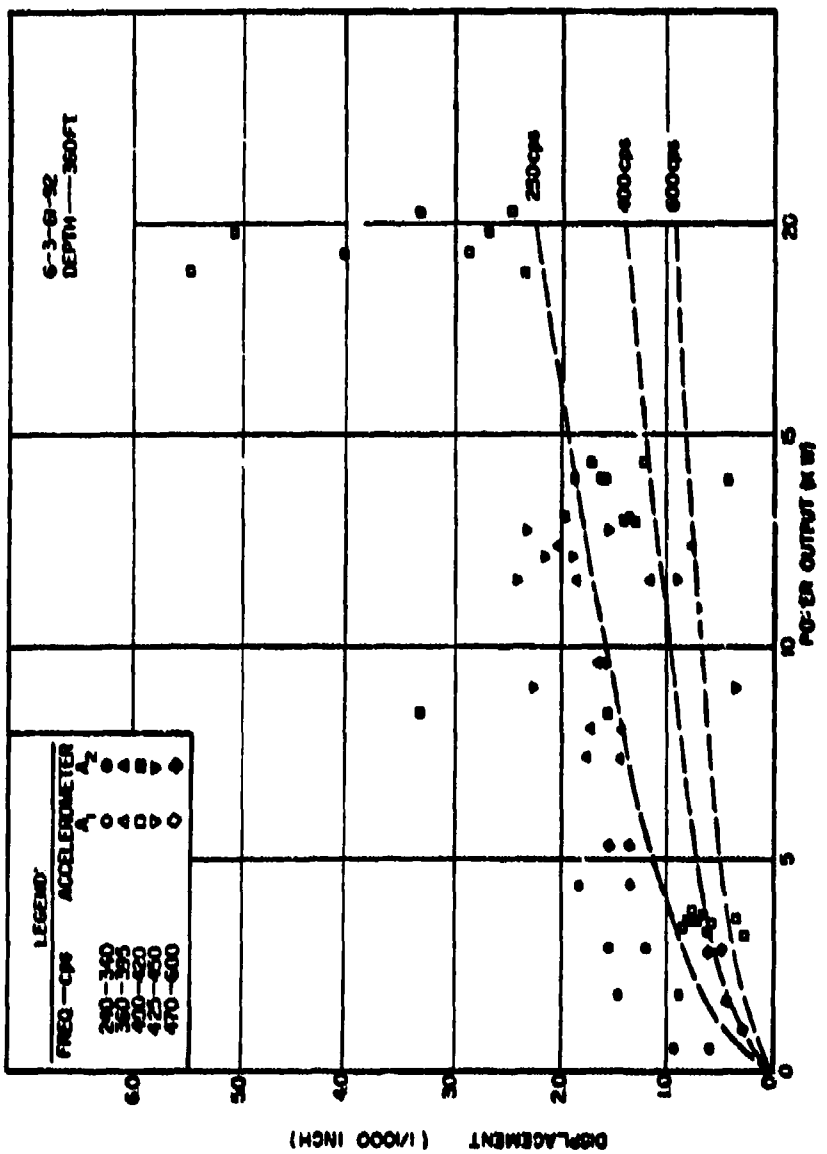

Figure 21 - Transducer displacement characteristics

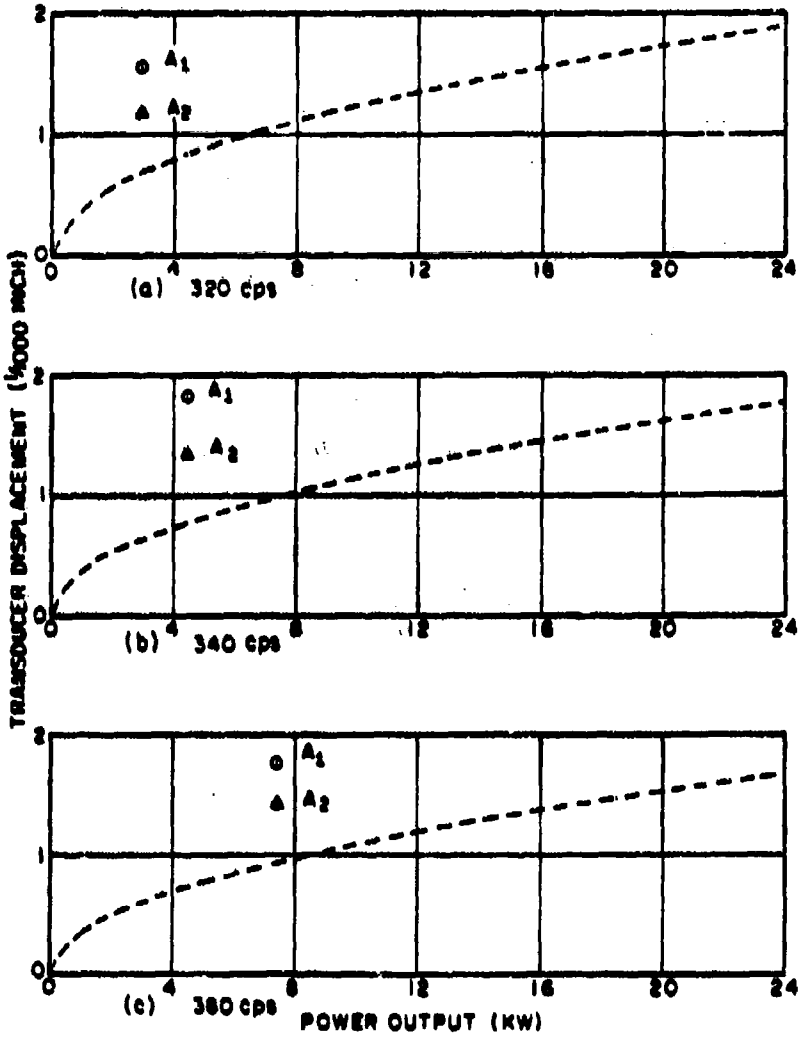

Figure 21 (Continued) - Transducer displacement characteristics

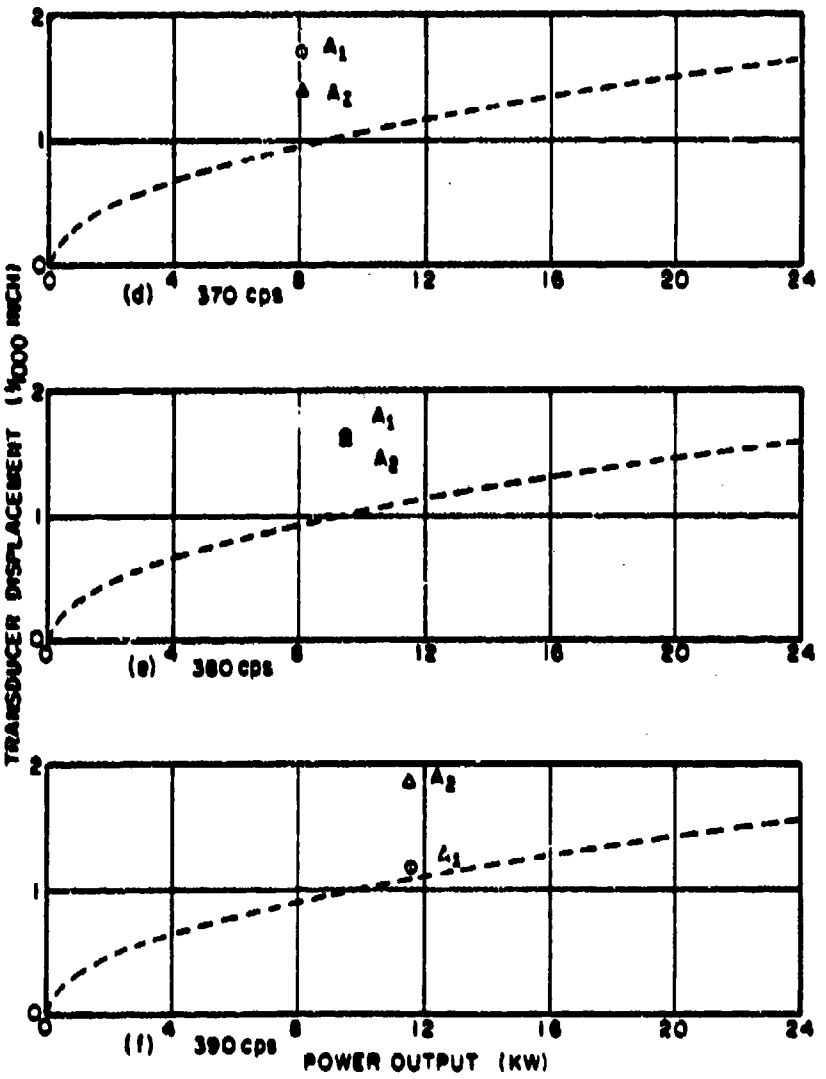

Figure 21 (Continued) - Transducer displacement characteristics

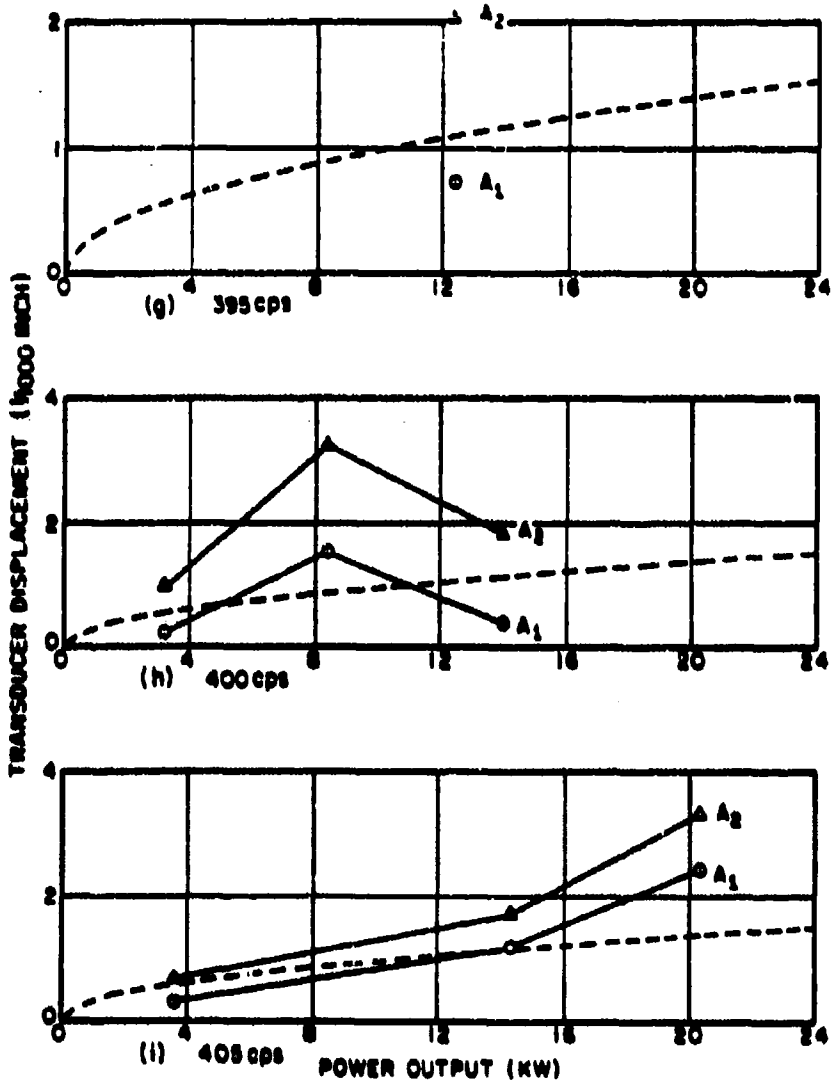

Figure 21 (Continued) - Transducer displacement characteristics

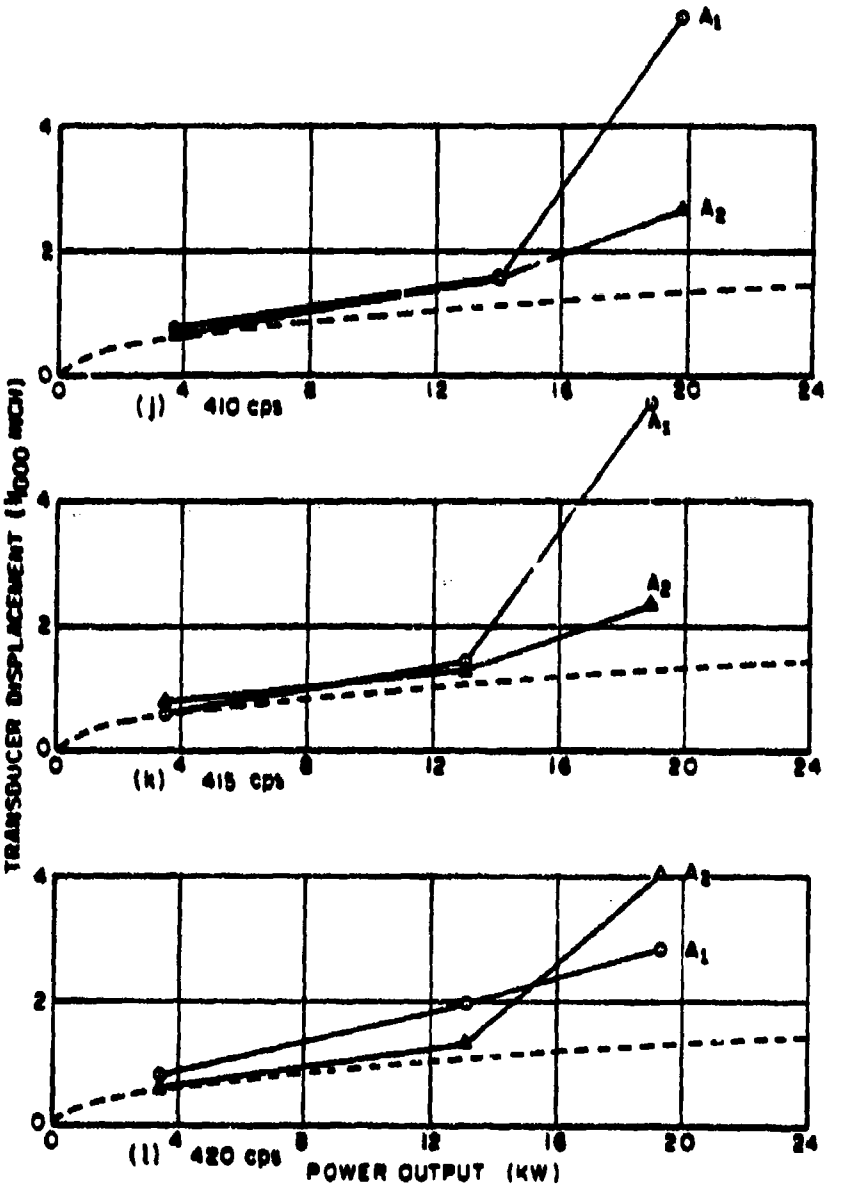

Figure 21 (Continued) - Transducer displacement characteristics

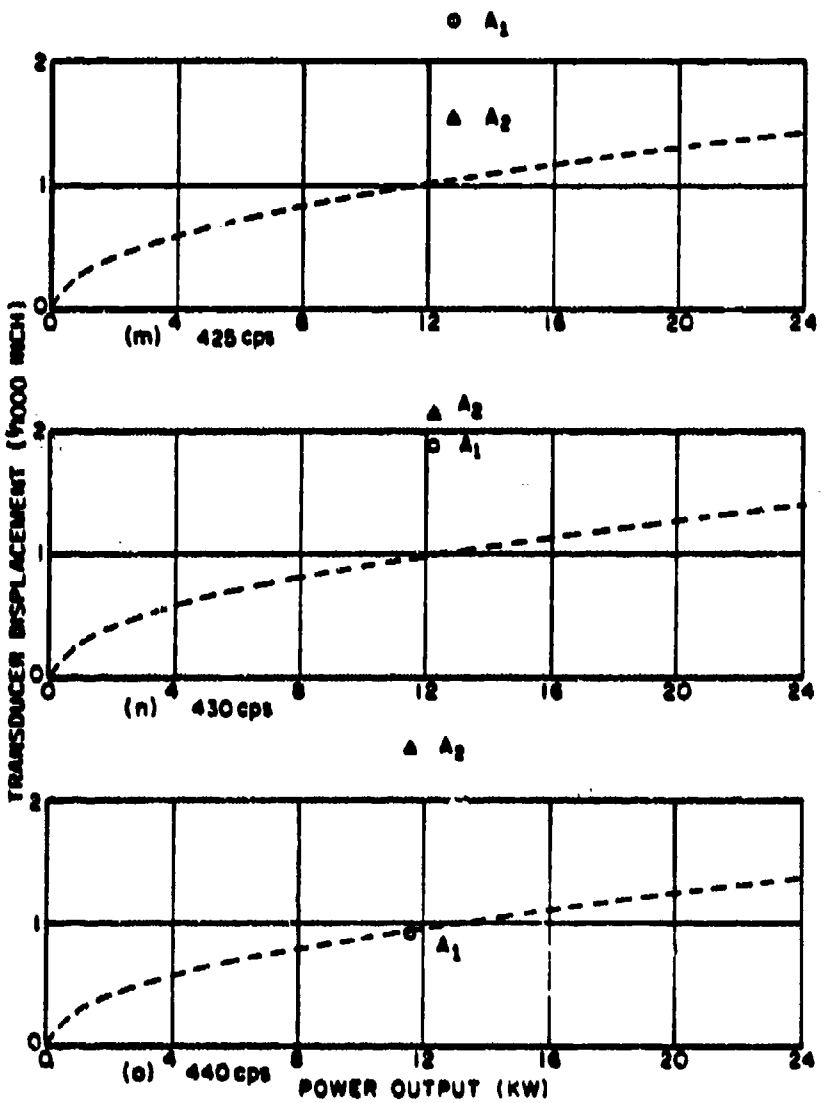

Figure 21 (Continued) - Transducer displacement characteristics

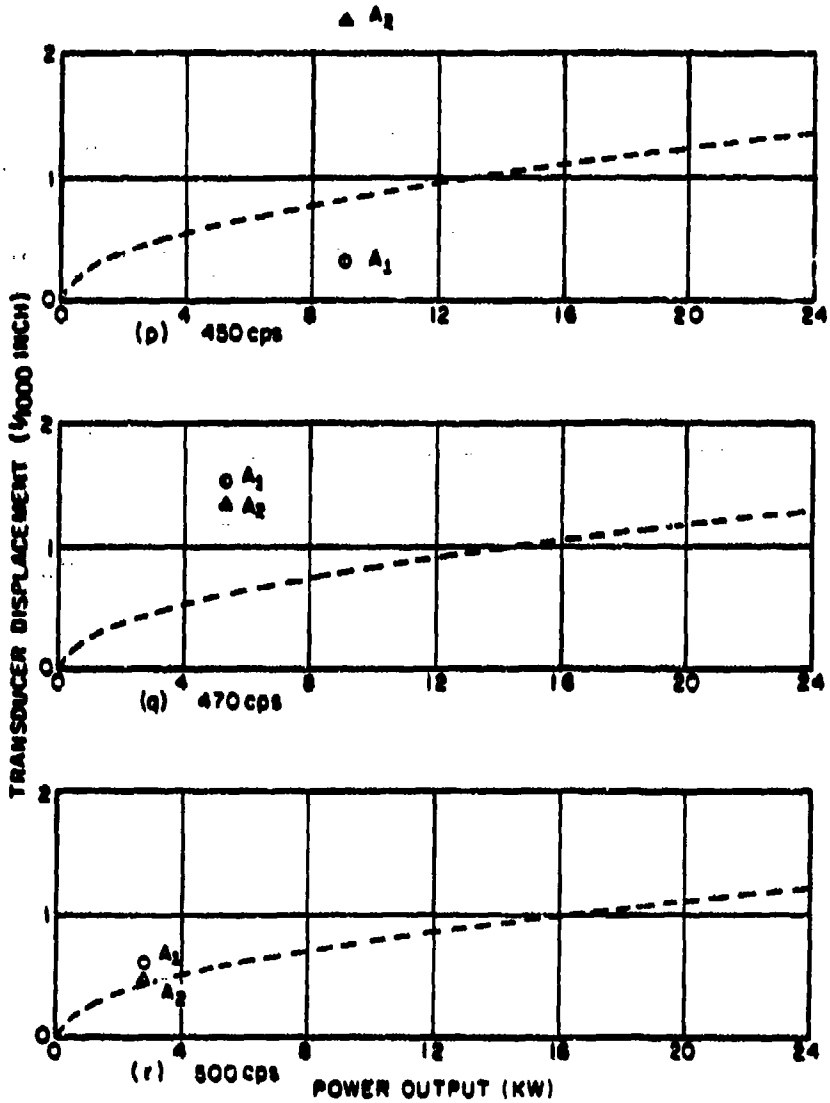

Figure 21 (Continued) - Transducer displacement characteristics

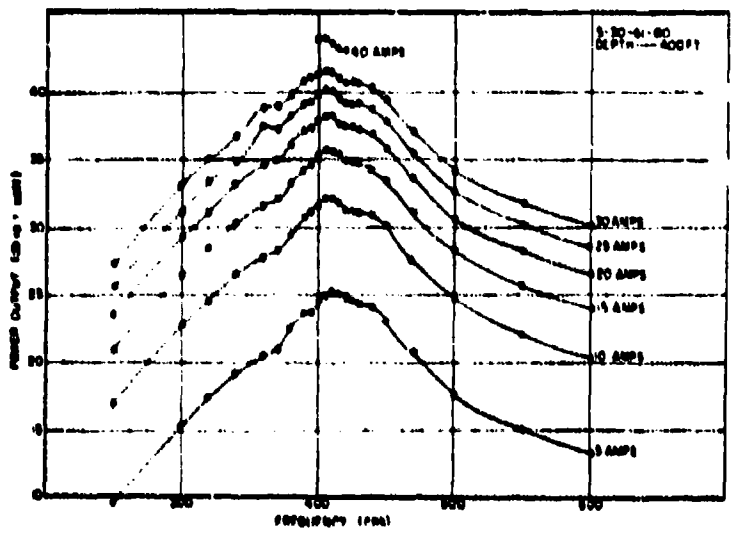

Figure 22 - Array response characteristics

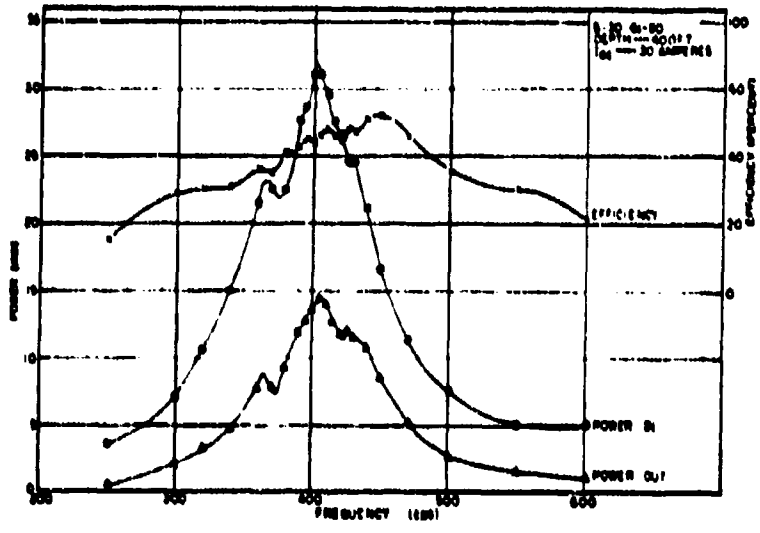

Figure 23 - Efficiency characteristics of array

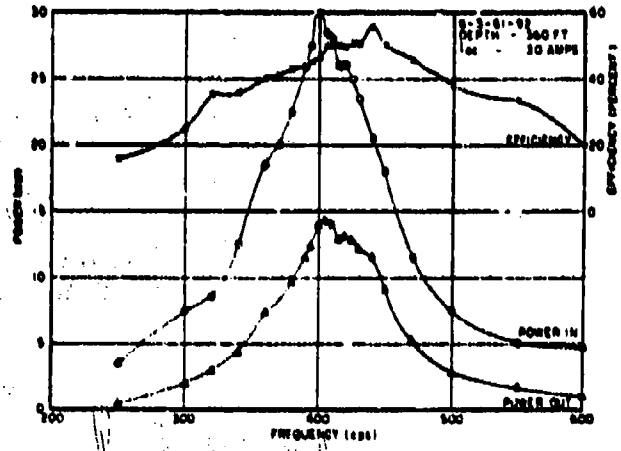

Figure 24 - Efficiency characteristics of array

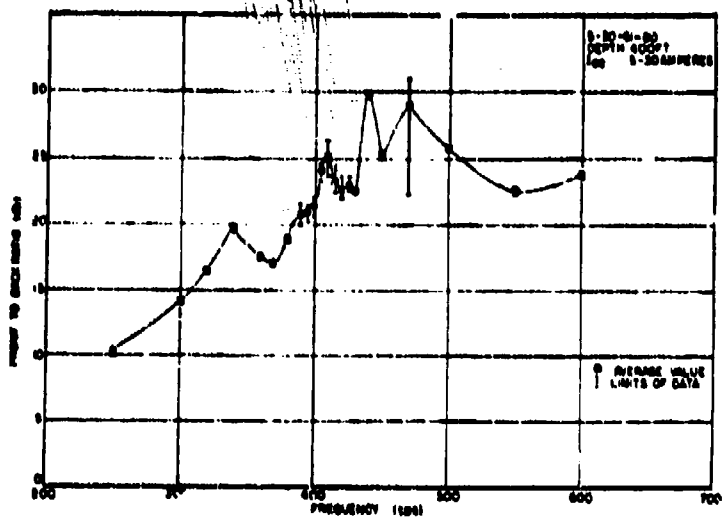

Figure 25 - Front to back discrimination

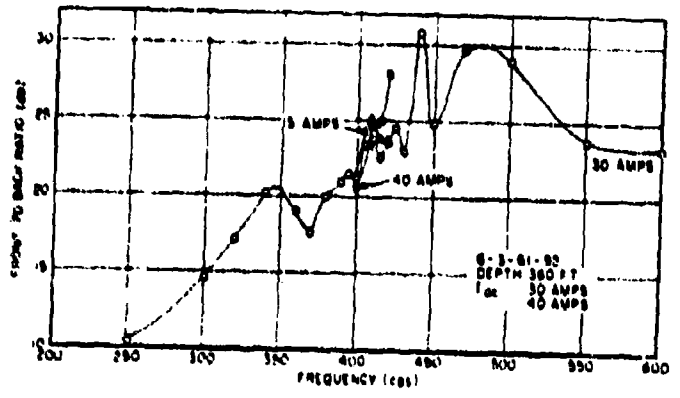

Figure 26 - Front to back discrimination

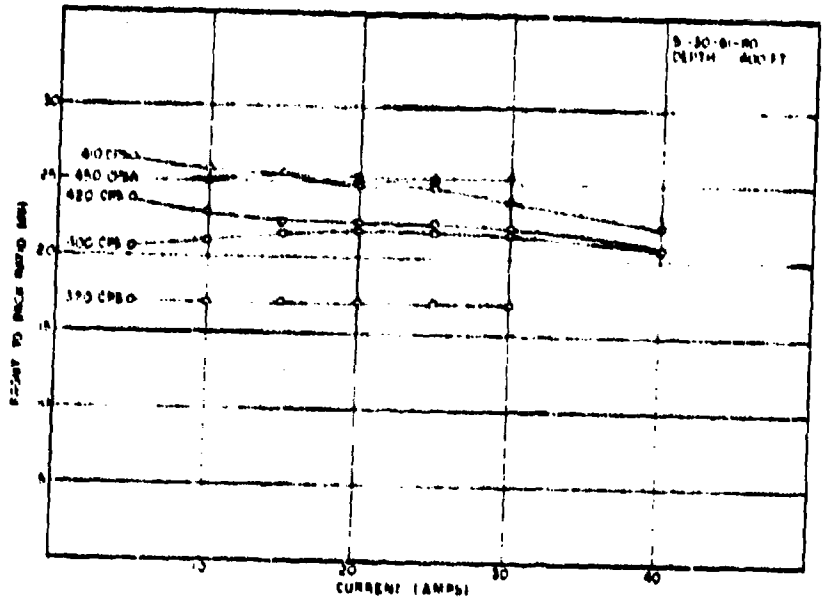

Figure 27 - Affect of current on front to back discrimination

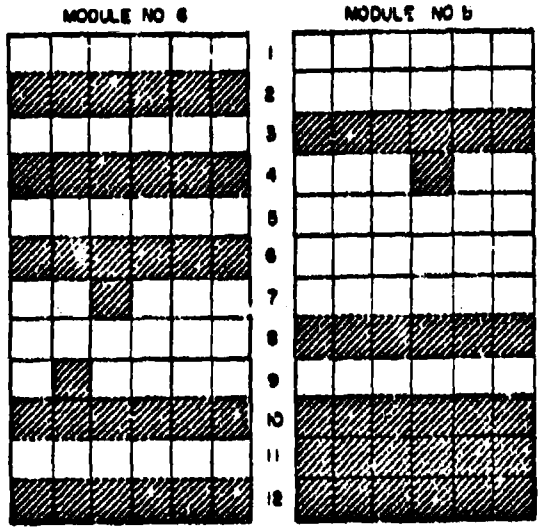

Figure 28 - Transducer replacement pattern of 22 May 1961

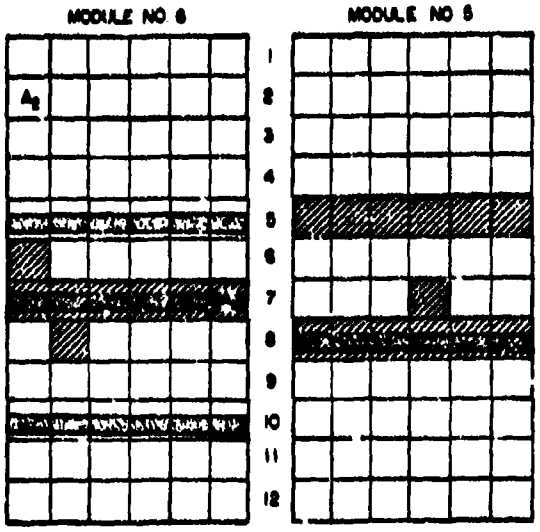

Figure 29 - Transducer and squash tube replacement pattern of 4 June 1961

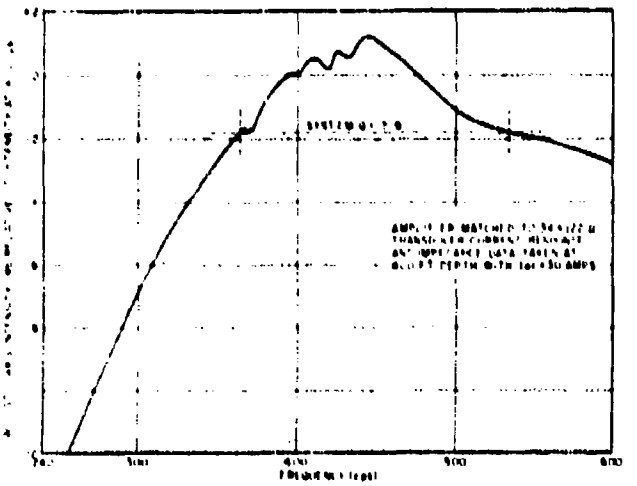

Figure 30 - System response for constant voltage input to amplifier

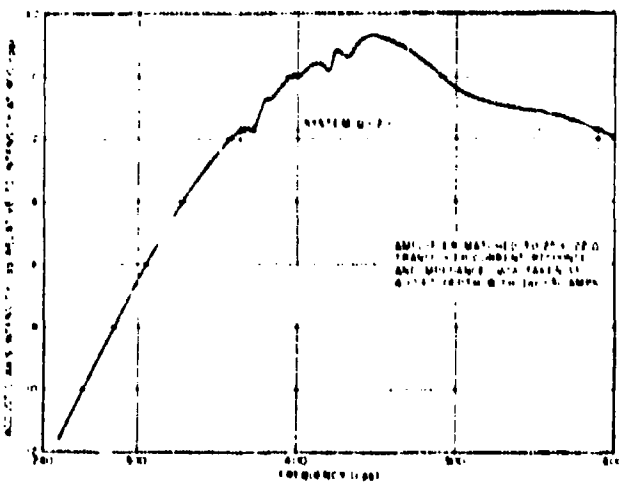

Figure 31 - System response for constant voltage input to amplifier

UNITED STATES GOVERNMENT

Memorandum

7100-016

DATE: 22 January 2004

REPLY TO ATTN OF: Burton G. Hurdle (Code 7103)

SUBJECT: REVIEW OF REF (A) FOR DECLASSIFICATION

TO: Code 1221.1

REF: (a) "Project ARTEMIS High Power Acoustic Source", A.T. McClinton, R.H. Ferris, W.A. Herrington, Sound Div., NRL Memo Report 1205, 3 Aug 1961 (U)
(b) "Project ARTEMIS High Power Acoustic Source Second Interim Report on Acoustic Performance", A.T. McClinton and R.H. Ferris, Sound Division, NRL Memo Report 1214, 19 September 1961 (U)
(c) "Project ARTEMIS High Power Acoustic Source Third Interim Report on Acoustic Performance", A.T. McClinton, R.H. Ferris, Sound Division, NRL Memo Report 1273, 23 April 1962 (U)
(d) "Project ARETMIS High Power Acoustic Source Effect of Transducer Element Electrical Connection on Interaction in a Consolidated Array", A.T. McClinton, Sound Division, NRL Memo Report 1323, 4 June 1962 (U)
(e) "Test of Project ARTEMIS Source", R.H. Ferris, Sound Division, NRL Memo Report 1648, 15 September 1965 (U)
(f) "Power Limitations and Fidelity of Acoustic Sources", R.H. Ferris and F.L. Hunsicker, Sound Division, NRL Memo Report 1730, November 1966 (U)
(g) "Project ARTEMIS Acoustic Source Acoustic Test Procedure", R.H. Ferris and C.R. Rollins, Sound Division, NRL Memo Report 1769, 5 June 1967 (U)
(h) "Calibration of the ARTEIS Source and Receiving Array on the Mission Capistrano", M. Flato, Acoustics Div., NRL Memo Report 2712, Dec 1973 (U)
(i) "Theoretical Interaction Computations for Transducer Arrays, Including the Effects of Several Different Types of Electrical Terminal Connections", R.V. Baier, Sound Division, NRL Report 6314, 7 October 1965 (U)
(j) "Project ARTEMIS Acoustic Source Summary Report", NRL Report 6535, September 1967 (U)

1. References (a) thru (j) are a series of reports on Project ARTEMIS Reports by the Sound Division that have previously been declassified.

2. The technology and equipment of reference (a) have long been superseded. The current value of these papers is historical

3. Based on the above, it is recommended that reference (a) be available with no restrictions.

Burton G. Hurdle

BURTON G. HURDLE
NRL Code 7103

CONCUR:

Edward R. Franchi 1/23/2004

E.R. Franchi Date
Superintendent, Acoustics Division

CONCUR:

Tina Smallwood 1/28/04

Tina Smallwood Date
NRL Code 1221.1